

# Design of a Robust Internal-loop Compensator of Clutch Positioning Systems

Jinsung Kim<sup>1</sup>, Seibum B. Choi<sup>1</sup>, Heerak Lee<sup>2</sup>, and Jaeuk Koh<sup>2</sup>

**Abstract**—This paper proposes a control scheme based on robust internal-loop compensator for a clutch positioning system. The purpose of control is to achieve a precise position control of automotive dry-clutch actuator system module. Overall system consists of the electric motor and the mechanical subsystem. A set of dynamic model is developed and validated experimentally. Robust internal-loop compensator is used to compensate unmodeled effect and unknown nonlinearities. Simulation and experimental results show that the proposed scheme has a better performance and tracking accuracy compared with simple PID controller.

## I. INTRODUCTION

There are various types of automatic transmissions such as conventional planetary-gear automatic transmissions (AT), automated manual transmissions (AMT), and dual clutch transmissions (DCT). Although ATs are the most popular system in the market, it may exhibit several limitations. ATs generally have a torque converter to transmit torque smoothly from the engine to wheels without abrupt change of torque fluctuation. But, it decreases the transmission efficiency significantly over gearshifting or engine idling. In addition, recent energy crisis and emission problems force transmission manufacturers have to meet the growing demands of improving fuel efficiency.

As a solution of this problem, dual clutch transmissions (DCTs) have received considerable attention in the last decade. Since DCTs have two power flow paths without a torque converter, control problems become quite challenging. Moreover, the use of dry-clutches makes a control more difficult in spite of high efficiency [1]. The use of electromechanical actuators is highly efficient, but its performance is sensitive to temperature variation [2]. Since the clutch engagement torque is highly sensitive to the stroke of the actuator, the position control quality of the clutch servo system determines the overall performance of DCTs. If there is a mismatch between the command from the transmission control unit and the actual position signal, the resulting clutch torque will be inaccurate. Thus, the clutch engagement performance is determined by how the control scheme robustly performs under several uncertainties. The position control of the clutch actuator should be as accurate as possible.

From this background, this paper considers the clutch positioning system for DCTs that plays the role in actuating

the clutch disk by an electric motor. The dynamic model of the clutch positioning system is proposed. Experimental validation of the model is also performed to find the system parameters. This control system has a force assistance mechanism that is highly nonlinear and uncertain. Moreover low sampling frequency for implementation is another obstacle to solve the problem. In order to overcome such limitations, the robust internal-loop compensator (RIC) is employed as a position controller that makes mechanical impedance of the actuator sufficiently large within a given specification. The RIC effectively rejects unknown disturbances to enable an uncertain system to behave like a nominal model. The outer controller is designed such that the system follows the desired position trajectory. Simulation and experimental results show the effectiveness of this approach. Since this study focuses on the actuator system for clutch positioning, it is assumed that desired clutch torque is calculated from the transmission control unit in advance. Thus, the desired actuator position trajectory is bounded and sufficiently smooth.

This paper is organized as follows. Section II introduces our application and the dynamic model. In Section III, a position controller is designed based on the robust internal-loop compensator. Simulation and experimental results are shown in Section IV and V, respectively. Section VI summarizes this paper.

## II. PROBLEM FORMULATION

### A. System Description

This section presents a brief description of the clutch positioning system for DCTs. Fig. 1 shows the clutch positioning system in the upper part, and the schematic of the model in the lower part. Basically, the system is driven by a brushless DC (BLDC) motor with a gear reducer. When the desired clutch position is commanded from the transmission control unit, it converted into the corresponding motor position. The controlled current drives the BLDC motor, and the motor torque is transformed into a rotational motion of a pinion gear through the gear reducer. The rack and pinion mechanism plays role of conversion of rotational-to-linear motion. The linear motion of the rack yields the carrier linear motion because the rack and carrier are attached together. The fork load is exerted at the end of the carrier. Therefore, the clutch positioning system should be controlled to follow the desired position while keeping a fork reaction load. Since this clutch positioning system is made for automatic transmissions without a torque converter particularly for DCTs, it is difficult to satisfy the transmission capability of the increased engine torque. As a solution of

<sup>1</sup>Jinsung Kim and Seibum B. Choi are with the Department of Mechanical Engineering, KAIST (Korea Advanced Institute of Science and Technology), Daejeon, Korea (jsk@kaist.ac.kr; sbchoi@kaist.ac.kr)

<sup>2</sup>Heerak Lee and Jaeuk Koh are with Valeo Pyeong Hwa Co, Ltd., Daegu, Korea (hrlee@vph.com; jaeuk.koh@vph.com)

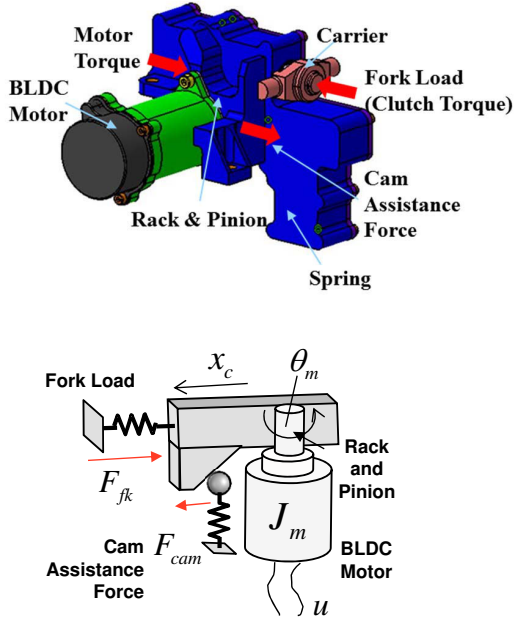


Fig. 1. Clutch positioning system for dual clutch transmissions

this problem, additional element is required to assist the limited motor torque. In Fig. 1, the cam feeder as a tool of a torque booster is inserted between the carrier and the actuator cover. The cam profile is suitably designed such that the feeder spring is applied to the carrier for reducing the motor power while the clutch positioning is carried out. But, nonlinear characteristics are mainly generated along the cam slide during motion. It may lead to deterioration of control accuracy significantly. Hence, a position controller, which will be designed, must have capability of compensation such nonlinearity.

### B. Dynamic Model

The actuator system is represented by the second order nonlinear dynamic model. The equations of motion shown in Fig. 1 are given as

$$J_m \dot{\omega}_m = k_m u - g_m \omega_m - T_L \quad (1)$$

$$T_L = r_p F_{fk}(x_c) - r_p F_{cam}(x_c) \quad (2)$$

where,  $J_m$  is the moment of inertia of motor,  $\omega_m$  the motor speed,  $\theta_m$  the motor position,  $k_m$  the motor torque constant,  $g_m$  the damping coefficient,  $r_p$  the radius of the pinion gear and  $u$  the motor current as a control input. The load torque  $T_L$  includes uncertain nonlinearities and unmodeled effect such as the cam assistance torque  $F_{cam}$ , and the fork load  $F_{fk}$  which are nonlinear function of the carrier position  $x_c$ . Since it is connected with the motor rotor, the following relationship can be obtained as

$$v_c = r_p \omega_m \quad (3)$$

$$\dot{x}_c = v_c \quad (4)$$

Note that (1) is rewritten as

$$J_m \dot{\omega}_m + g_m \omega_m = k_m u - r_p F_{fk}(x_c) + r_p F_{cam}(x_c). \quad (5)$$

The operating region of interest is from the contact point of the clutch to desired position that corresponds to the desired clutch torque. This operating range is approximated by linear stiffness model for the control purpose. Therefore, (2) is linearly parameterized as

$$\bar{F}_{fk}(x_c) = \bar{k}_{cam} x_c = \bar{k}_{cam} r_p \theta_m \quad (6)$$

$$\bar{F}_{cam}(x_c) = F_{fk0} + \bar{k}_{fk} x_c = F_{fk0} + \bar{k}_{fk} r_p \theta_m \quad (7)$$

where,  $\bar{F}_{fk}$  and  $\bar{F}_{cam}$  denote the approximated fork load and the cam assistance force,  $\bar{k}_{fk}$  and  $\bar{k}_{cam}$  the stiffness of the fork and the cam within the operation range. Substituting (6) and (7) into (1), the following model can be obtained as

$$J_m \dot{\omega}_m = k_m u - g_m \omega_m - r_p \bar{F}_{fk}(x_c) + r_p \bar{F}_{cam}(x_c) + d \quad (8)$$

where  $d$  is a lumped disturbance including linearization error and unmodeled effect.

The effect of the cam feeder spring shown in Fig. 1 needs to be investigated. To reduce the required motor power, the stiffness of the cam feeder spring  $\bar{k}_{cam}$  can be further increased in this system. If  $\bar{k}_{cam}$  is increased from the nominal value, a real pole of the system moves toward the origin. It is possible that there are some values of  $\bar{k}_{cam}$  to make one of poles enter into the right half plane, which implies that the system becomes unstable. Although the proportional-integrative-derivative (PID) control is simply available, it may lead to instability of the closed-loop system due to the limited bandwidth of the open-loop system as well as some unmodeled uncertainties.

In the clutch actuator system in automotive transmissions, a clutch actuator should be required to cover a large frequency bandwidth in order to have quick response corresponding to the gear-shift command. To achieve such a goal without large stiffness of the cam feeder spring and an increased driving torque requirement of the motor, a robust control scheme has to be developed within a given specification. It will be discussed in the next section.

### C. Parameter Identification

To analyze the system behavior and design a position controller, the parameters of the developed model needs to be identified. This process involves two steps for motor dynamics and the load torque parts. First, the linear system part for motor dynamics is identified without considering the load torque  $T_L$ . To decouple linear parts from entire system dynamics, it is assumed that the last three terms in the right hand side are neglected in (8) at this stage. The BLDC motor at the experimental system is disconnected from the mechanical actuator part so that the original system (8) is written as  $J_m \dot{\omega}_m = k_m u - g_m \omega_m$ , and the transfer function forms are represented as

$$P_n^\omega(s) = \frac{\omega_m(s)}{u(s)} = \frac{k_m}{J_m s + g_m} = \frac{k'_m}{\tau s + 1} \quad (9)$$

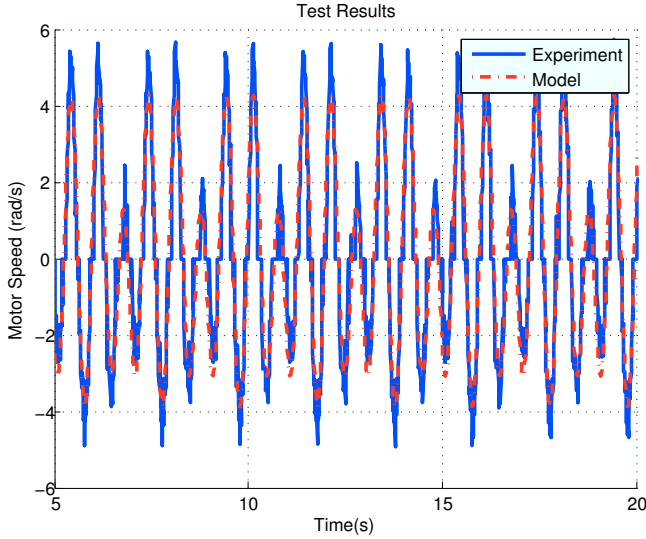


Fig. 2. Sinusoidal input validation of the identification result.

$$P_n^\theta(s) = \frac{\theta_m(s)}{u(s)} = \frac{k_m}{J_m s + g_m} = \frac{k'_m}{\tau s^2 + s} \quad (10)$$

where  $\tau = J_m/g_m$  and  $k'_m = k_m/g_m$ . Note that (9) is the transfer function from the motor current to the speed, and (10) is the one for the current to the position, respectively. In this formulation, the parameters  $J_m$ ,  $g_m$ , and  $k_m$  need to be estimated. The available measurements are the control input  $u$  and the motor position  $\theta_m$ , and the motor speed  $\omega_m$ .

The parameter identification process is formulated as the following optimization problem:

$$\hat{\Theta} = \arg \min_{\Theta} \frac{1}{N} \sum_{k=1}^N [y(k) - \hat{y}(k, \Theta)]^2 \quad (11)$$

where,  $k$  is the time instant in the discretized system of (9),  $y = [u, \theta_m, \omega_m]^T$  the measurement vector,  $\Theta = [J_m, k_m, g_m]^T$  the unknown parameter vector. To solve this problem, an appropriate input signal is required such that the system satisfies persistence of excitation condition [3]. Pseudo random binary noise signal (PRBS) is used to overcome nonlinear frictional effect that is not modeled in the linear part of the model. Then, the sinusoidal input signal having several frequency components is applied to the motor system for validation of the identification result by PRBS.

There are several techniques for parameter identification of dynamic systems. In this study, nonlinear least-square method is employed to find parameters of our system. The resulting identified parameters via PRBS are  $J_m = 0.0106 \text{ kgm}^2$ ,  $k_m = 1.9294 \text{ Nm/A}$ ,  $g_m = 1.1850 \text{ Nm sec}$ . These parameters are validated by sinusoidal input as shown in Fig. 2.

#### D. Control Objective

The control objective of this paper is to design a position controller of clutch servo-actuator in automotive systems in spite of the presence of uncertainties. The position tracking error  $e_m$  is defined as  $e_\theta := \theta_{md} - \theta_m$ . with a given

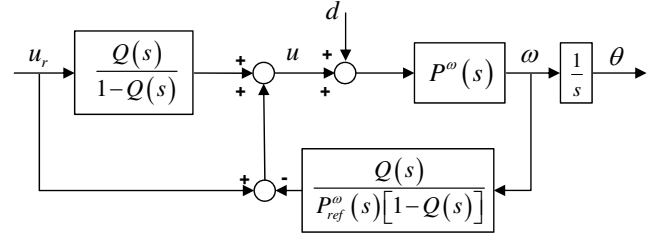


Fig. 5. Block diagram of the disturbance observer.

desired motor position trajectory  $\theta_{md}$ . In the subsequent development, the controller plays role in regulating the tracking error  $e_\theta$ .

### III. CONTROLLER DESIGN

#### A. Overview of Robust Inner-loop Compensator

In many engineering systems, there will always exist unmeasurable disturbances. The disturbance observer (DOB) is well-known approach to estimate and reject modeling uncertainties and disturbances [4], [5]. In the DOB formulation shown in Fig. 5, the nominal model of the plant is used to estimate disturbance. Briefly, estimated disturbance can be obtained by which the difference between the inverse of the nominal model multiplied by outputs and inputs can be filtered through a low-pass filter  $Q(s)$  called Q-filter. The bandwidth of the Q-filter is determined the frequency range of a given plant system.

Particularly in a position control of mechanical systems, two degree-of freedom (DOF) design is preferred because a pre-filter  $F(s)$  is applicable to make an uncertain system  $P^\omega(s)$  with disturbance become a reference system  $P_{ref}^\omega(s)$  [5]. The structure of two DOF design is shown in Fig. 3. The transfer function  $G_{\omega_r, \omega}$  from the reference input to the system output is given as

$$G_{\omega_r, \omega}(s) = F(s) \frac{P^\omega(s)K(s)}{1 + P^\omega(s)K(s)} \quad (12)$$

When the prefilter  $F(s)$  is designed such that  $|G_{\omega_r, \omega}(s)| = 1$ , an uncertain system  $P^\omega(s)$  behaves like a reference system  $P_{ref}^\omega(s)$ . Therefore,  $F(s)$  can be chosen as

$$F(s) = \left[ \frac{P_{ref}^\omega(s)K(s)}{1 + P_{ref}^\omega(s)K(s)} \right]^{-1}. \quad (13)$$

After some algebraic manipulation, the configuration of the control system in Fig. 3 is converted into Fig. 4, equivalently. The control formulation in Fig. 4 is called the robust internal-loop compensator (RIC) that is an advanced motion controller that provides the enhanced robustness and transient performance [6]–[8]. Note that RIC has structural equivalence with disturbance observer (DOB) approach. In Fig. 4, the control input  $u$  is defined as

$$u = u_r + K(s)e_\omega \quad (14)$$

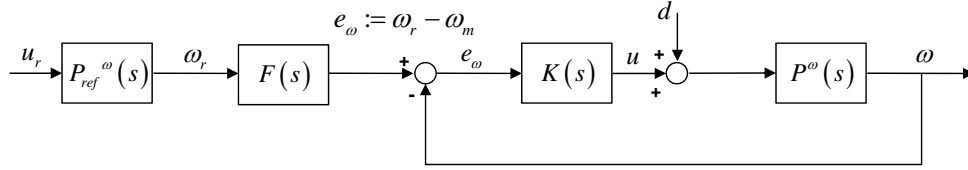


Fig. 3. Block diagram of the two degree-of-design.

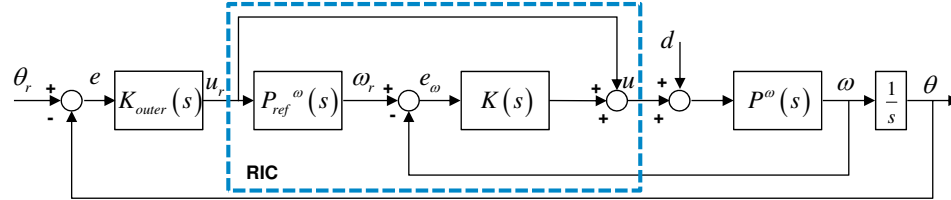


Fig. 4. Block diagram of the robust internal-loop compensator.

where  $u_r$  is the feed-forward input, and  $e_\omega$  is the speed control error  $e_\omega := \omega_{md} - \omega_m$ . The transfer function from input  $u$  and the motor speed  $\omega_m$  is given as

$$\omega_m(s) = \frac{P^\omega(s)}{1 + P^\omega(s)K(s)} [(1 + P_{ref}^\omega(s)K(s))u_r + d]. \quad (15)$$

It should be noted that two DOF design, DOB, and RIC have structural equivalence [8]. This property provides a guide on how to select a prefilter  $F(s)$ . It is desirable that  $F(s)$  can be also designed as the inverse of Q-filter, i.e.  $F(s) = [Q(s)]^{-1}$ . With this and (13),  $Q(s)$  is written as

$$Q(s) = \frac{P_{ref}^\omega(s)K(s)}{1 + P_{ref}^\omega(s)K(s)}. \quad (16)$$

Now, the structure of the Q-filter (16) is taken into account as a first-order filter with the time constant  $\tau_Q$ :

$$Q(s) = \frac{1}{\tau_Q s + 1} \quad (17)$$

From the DOB formulation in Fig. 5, the transfer function (15) can now be rewritten as

$$\omega_m(s) = [P_{no}^\omega(s)u_r + P_{no}^\omega(s)(1 - Q(s))d] \times \frac{P^\omega(s)}{P_{no}^\omega(s) + [P^\omega(s) - P_{no}^\omega(s)]Q(s)} \quad (18)$$

where  $P_{no}^\omega(s)$  is a nominal model of the plant (9).

### B. Design of a RIC-based Controller

In our system, the nominal model  $P_{no}^\omega(s)$  can be approximated as

$$P_{no}^\omega(s) = \frac{k'_{m0}}{\tau_0 s + 1} \quad (19)$$

Substituting (16) into (18) with setting  $P_{no}^\omega(s) = P_{ref}^\omega(s)$  yields the transfer function which is the same as (15). This equivalence shows the feasibility of (16), and it can be

rewritten with respect to the feedback compensator gain  $K(s)$  as the following

$$K(s) = \frac{Q(s)}{1 - Q(s)} [P_{no}^\omega(s)]^{-1} = \frac{1}{\tau_Q s} \frac{\tau_0 s + 1}{k'_{m0}} = K_p + K_i \frac{1}{s} \quad (20)$$

where  $K_p$  and  $K_i$  are control gains of  $K(s)$  defined as

$$K_p := \frac{\tau_0}{\tau_Q k'_{m0}}, \quad K_i := \frac{1}{\tau_Q k'_{m0}}. \quad (21)$$

Note that the resulting control gains of  $K(s)$  is proportional-integrative (PI) type. Such gains are determined on the system dynamics of the nominal system and the design parameter  $\tau$  so that the gain design procedure of the internal controller is systematic.

Similarly with the DOB design case, the internal controller has large bandwidth as  $\tau_0$  is increased. In general, the choice of small  $\tau_0$  is advantageous in order to enhance robustness of the controller. However, since the motor bandwidth and the sampling frequency of the controller is limited, the optimal value of  $\tau_0$  should be chosen carefully.

The next step is to design an outer loop controller which corresponds to  $K_{outer}(s)$  in Fig. 4. A proportional-derivative (PD) controller is employed to make the error  $e_\theta$  converge to zero. Hence,  $K_{outer}(s)$  is chosen as

$$K_{outer}(s) = K_{pout} + K_{dout} s \quad (22)$$

where  $K_{pout}$  and  $K_{dout}$  are control gains of  $K_{outer}(s)$ . As shown in Fig. 4, the velocity tracking error is controlled by  $K(s)$  in the internal-loop while the position measurement is fed back into the outer controller only. Since the reference speed trajectory is calculated from the reference model, uncertainties and disturbances are internally compensated by  $K(s)$  and additional feed-forward  $u_r$ . The resulting control bandwidth is increased.

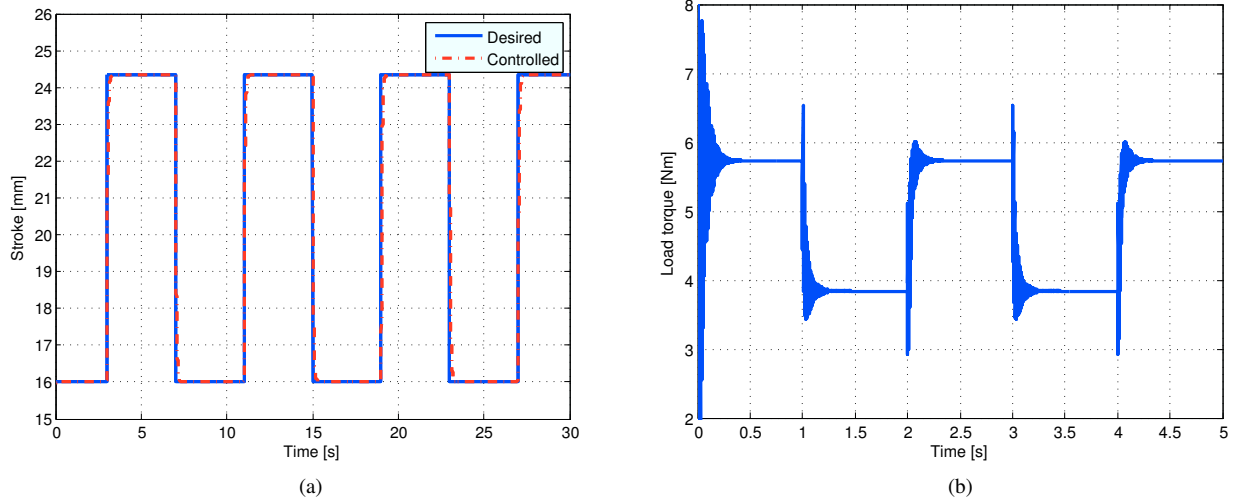


Fig. 6. Simulation results of the RIC-based controller with  $\tau_0 = 0.01$  and square wave profile: (a) Position tracking result, (b) Applied load torque to the motor.

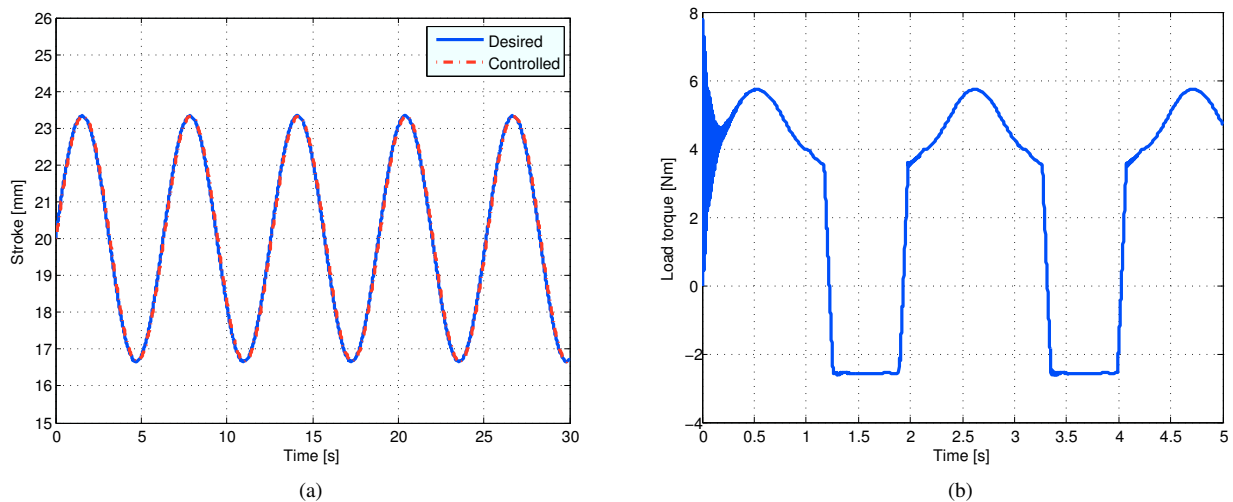


Fig. 7. Simulation results of the RIC-based controller with  $\tau_0 = 0.01$  and sine wave profile: (a) Position tracking result, (b) Applied load torque to the motor.

#### IV. SIMULATION RESULTS

The simulations are performed to demonstrate the control design developed in the preceding section. Desired position trajectory is defined as square wave form. Although a step-like position profile is not necessary in practice, this configuration can impose the worst case of the working condition. Simulations are performed under the assumption that the fork load, which corresponds to the clutch torque, is applied to the positioning system. The magnitude of the position corresponds to the stroke of the carrier having the full engagement torque from the kissing point. The nominal model  $P_{ref}^\omega(s)$  of the RIC framework is chosen as (9).

Fig. 6 shows the tracking control results by the RIC-based controller when applying the square wave profile. The design parameters are selected as  $\tau_0 = 0.01$ ,  $K_{pout} = 28$ ,  $K_{dout} = 0.06$ . In Fig. 6(a), the result shows that the controller works well. Fig. 6(b) shows the applied load torque to the motor

that caused by all uncertainties and disturbances.

Fig. 7 shows the case of the sine wave profile. The design parameters are selected as  $\tau_0 = 0.01$ ,  $K_{pout} = 120$ ,  $K_{dout} = 0.06$ . In Fig. 7(a), the precise position control is achieved. In Fig. 7(b), asymmetric load torque can be observed. This behavior is due to the cam assistant spring force and nonlinear friction in the mechanical part of the system. It shows that the proposed controller can effectively reject nonlinear disturbances in Fig. 7(b).

#### V. EXPERIMENTAL RESULTS

The experimental setup is shown in Fig. 8. The controller is implemented by using dSPACE MicroAutoBox (MABX) that is a rapid control prototyping board. The sampling frequency is 100 Hz that is the same environment of the actual vehicle configuration. In Fig. 8, transmission power unit (TPU) is a motor amplifier to obtain the required current

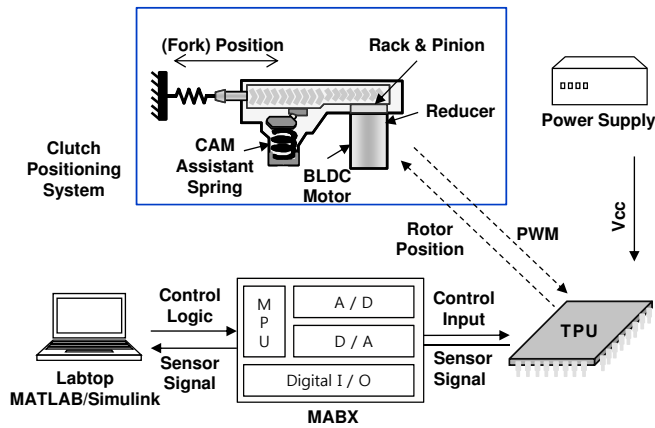


Fig. 8. Schematic of the experimental setup

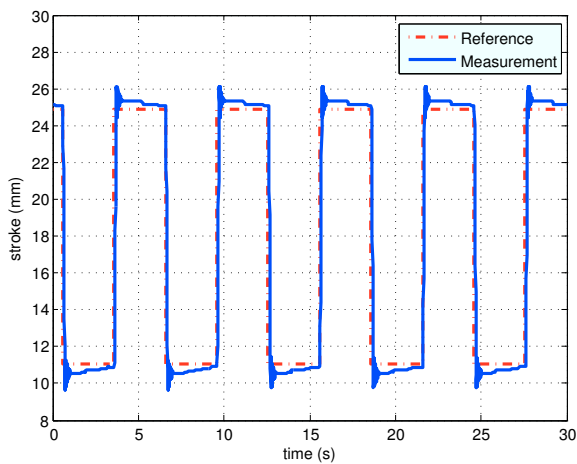


Fig. 9. Experimental result of the PID controller: Position tracking result

level. Signals on the overall control system are transmitted by controller area network (CAN) along the bus line.

For a performance comparison, the experimental result of PID controller shown in Fig. 9. The resulting position trajectory has some overshoot and steady-state error. As mentioned before, the system bandwidth is limited due to the cam assistance force and the sampling frequency. Hence, repeated tuning process does not overcome this problem. Fig. 10 shows the experimental result of the RIC. Compared with the result of the PID controller in Fig. 9, the proposed method shows better tracking performance. The design parameters for the RIC are chosen as  $\tau_0 = 0.01$ ,  $K_{pout} = 11$ ,  $K_{dout} = 0.04$ .

## VI. CONCLUSION

This paper proposes a robust controller for clutch positioning system for dual clutch transmission. Since an electromechanical device is utilized to drive the mechanical part of the actuator within a given specification, a control strategy is needed to overcome limited operating condition. Based on the dynamic model with experimental validation, the RIC based position controller is designed such that it can successively reject unknown disturbances. As a result,

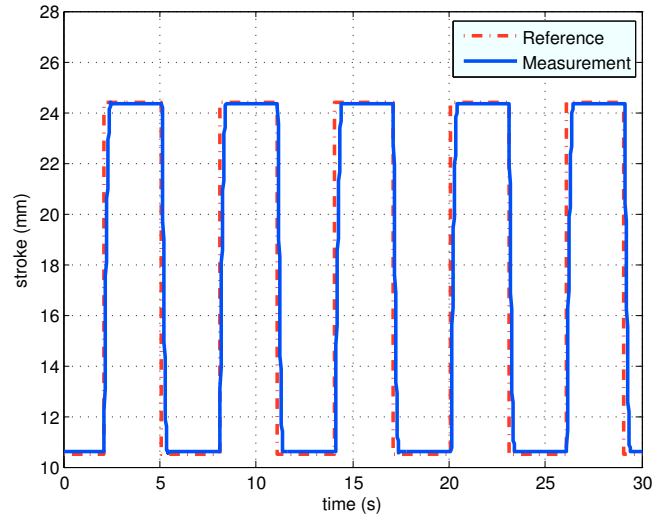


Fig. 10. Experimental result of the RIC-based controller: Position tracking result

the driving motor has a wide frequency bandwidth for clutch control. Simulation and experimental results show the effectiveness of the RIC-based position controller. In future works, a feed-forward controller can be added to the current control framework by considering nonlinear friction model and parameter adaptation approach. Also, the modeling of the cam assistance force and the fork load characteristics will be elaborated.

## REFERENCES

- [1] P. Dolcini, C. Canudas de Wit, and H. B echart, "Lurch avoidance strategy and its implementation in AMT vehicles," *Mechatronics*, vol. 18, no. 5-6, pp. 289-300, June 2008.
- [2] A. J. Turner and K. Ramsay, "Review and development of electromechanical actuators for improved transmission control and efficiency," SAE, Tech. Rep. 2004-01-1322, 2004.
- [3] L. Ljung, *System Identification: Theory for the User*, ser. Prentice-Hall information and system sciences series. Englewood Cliffs, NJ: Prentice-Hall, 1987.
- [4] K. Ohnishi, "A new servo method in mechatronics," *Transactions of Japanese Society of Electrical Engineers*, vol. 107, no. D, pp. 83-86, 1987.
- [5] T. Umeno, T. Kaneko, and Y. Hori, "Robust servosystem design with two degrees of freedom and its application to novel motion control of robot manipulators," *IEEE Trans. Ind. Electron.*, vol. 40, no. 5, pp. 473-485, oct. 1993.
- [6] B. K. Kim, W. K. Chung, H.-T. Choi, I. H. Suh, and Y. H. Chang, "Robust internal loop compensator design for motion control of precision linear motor," in *Industrial Electronics, 1999. ISIE '99. Proceedings of the IEEE International Symposium on*, vol. 3, 1999, pp. 1045-1050 vol.3.
- [7] B. K. Kim and W. K. Chung, "Unified analysis and design of robust disturbance attenuation algorithms using inherent structural equivalence," in *American Control Conference, 2001. Proceedings of the 2001*, vol. 5, 2001, pp. 4046-4051 vol.5.
- [8] —, "Advanced disturbance observer design for mechanical positioning systems," *IEEE Trans. Ind. Electron.*, vol. 50, no. 6, pp. 1207-1216, dec. 2003.